Safeguarding Cultural Heritage: Integrative Analysis of Gravitational Mass Movements at the Mortuary Temple of Hatshepsut, Luxor, Egypt.

Benjamin Jacobs[1], Mohamed Ismael[2,3], Mostafa Ezzy[2,3], Markus Keuschnig[4], Alexander Mendler[5],
5 Johanna Kieser[1], Michael Krautblatter[1], Christian U. Grosse[5], Hany Helal[2,3].

[1]Chair of Landslide Research, TUM School of Engineering and Design, Technical University of Munich, Munich, Germany
[2]Department of Mining, Petroleum, and Metallurgical Engineering, Faculty of Engineering, Cairo University, Giza, Egypt
[3]UNESCO Chair on Science and Technology for Cultural Heritage, Faculty of Engineering, Cairo University, Giza, Egypt
[4]GEORESEARCH Research Institute, Wals, Austria
10 [5]Chair of Non-destructive Testing, TUM School of Engineering and Design, Technical University of Munich, Munich, Germany

Correspondence to: Benjamin Jacobs (benjamin.jacobs@tum.de)

Abstract. The 3500 years old Mortuary Temple of Hatshepsut with its unique architecture is a key Egypt Cultural Heritage Site and the best-preserved temple in Deir El-Bahari (Luxor, Egypt). The neighbouring temple of Thutmose III in a similar

15 geological setting was buried by a major historic rock slope failure originating from the 100 m vertical limestone cliff behind the Deir El-Bahari temple complex. The project "High-Energy Rockfall ImpacT Anticipation in a German Egyptian cooperation (HERITAGE)" aims to use gravitational mass movement hazard analyses, Terrestrial Laser Scanning (TLS) and Interferometric Synthetic Aperture Radar (InSAR) for deformation and topographic change analysis, ambient vibration analyses, and rockfall runout modelling of potential failures to systematically assess rockfall hazards. The non-invasive nature

20 of our methods is crucial for safeguarding cultural heritage, as it allows for monitoring without physical contact with the site, preserving both the integrity and the safety of historically significant areas. This study is one of the first to transfer and integrate well-established monitoring techniques from mountainous areas to Egyptian World Heritage Sites.

HERITAGE is a cooperation between the Technical University of Munich (TUM) and Cairo University (CU) focusing on the analysis and assessment of the rock slope stability behind the archaeological heritage in Deir El-Bahari. Here we show the

25 remarkable potential of transferring established methods from mountainous regions to a world-famous cultural heritage site. We demonstrate the capabilities of our integrated approach in a challenging climatic, geomorphological and archaeologically sensitive environment, and produce the first event and impact analysis of gravitational mass movements at the Temple of Hatshepsut, providing vital data towards future risk assessment.

1. Introduction

Gravitational mass movements can pose a significant threat to infrastructure and people worldwide. While their role on infrastructure in mountain regions worldwide has been emphasized in many publications, their long-term-impact on cultural heritage has been poorly addressed so far. Here we report the impact of rockfalls and rock slope failure over 3 millennia at the Mortuary Temple of Hatshepsut, a top-level cultural heritage site, nestled at the base of the Theban Hills in Deir El-Bahari, Luxor. The Temple of Hatshepsut, an engineering marvel from the fifteenth century BC dedicated to the worship of Amon and Hathor, exhibits a unique architectural integration with Gebel Gurnah's rock mass, featuring ca. 100 m high, (sub-)vertical cliffs with prominent rock tower structures (Figure 1). Due to its priceless historic value the Temple of Hatshepsut is part of the UNESCO World Heritage Site of Ancient Thebes with its Necropolis (UNESCO World Heritage, 2025).

Geological and geomorphological studies indicate historic gravitational collapses in the Deir El-Bahari valley, with archaeological evidence of a significant rockfall in 1100–1080 B.C., attributed to an earthquake, which destroyed the temple of Thutmose III (Karakhanyan et al., 2010). Modern instances, such as the 1985 rockfall event near Temple of Hatshepsut (Abdallah and Helal, 1990), underscore the ongoing risk.

The Deir El-Bahari cliffs demand a nuanced understanding to safeguard the temple and its visitors. Despite the historical importance of the site, research on the stability of the surrounding the Temple of Hatshepsut is limited to the neighbouring Valley of Kings (Alcaíno-Olivares et al., 2019; Marija et al., 2022), are restrained to the geological past (Dupuis et al., 2011) and focus more on general risk potential rather than active hazard process monitoring (Chudzik et al., 2022; Marija et al., 2022; Abdallah and Helal, 1990).

While remote techniques have boosted in the last decade in Alpine Environments, their applicability to delimit and anticipate rock instability in world heritage sites with different climatological and seismic conditions, and rock sequences with a significantly lower mechanical strength in comparison to Alpine rock walls, has not been tested. In a benchmark field study, we tested near vertical slopes with a combination of multi-temporal terrestrial laser scanning (TLS) and satellite-based interferometric synthetic aperture radar (InSAR), both non-invasive measurement methods well-suited for protected sites, to characterise rock wall geometry, potential volumes and deformations. Based on this and historical information, we used numerical runout modelling including historical scenarios. Ambient vibration measurements were applied to investigate their potential to detect internal weakening and deformations prior to the accuracy level of optical and radar measurements.

TLS offers rapid and accurate remote data acquisition for large and inaccessible areas, crucial for characterizing rock slopes and conducting 3D change detection (Abellán et al., 2014). The capabilities of TLS in terms of gravitational hazard monitoring and rockfall quantification have been extensively demonstrated in the past (Santos Delgado et al., 2009; Matasci et al., 2018; Hartmeyer et al., 2020; Draebing et al., 2022; Strunden et al., 2015) therefore its application at this potential risk site is adequate.

InSAR has proven to be a powerful tool in geotechnical and geological studies, particularly for monitoring land deformation and assessing slope stability in challenging environments (Intrieri et al., 2018; Carlà et al., 2019). Its application extends to

various cultural heritage sites, where traditional methods may be restricted due to the need to preserve sensitive structures. For instance, InSAR has been effectively used to detect subsidence and ground movement around ancient structures, such as the

65 Leaning Tower of Pisa (Solari et al., 2016; Falco et al., 2022) and archaeological sites in Petra, Jordan (Margottini et al., 2017) highlighting its utility in identifying early warning signs of potential hazards. The non-invasive nature of InSAR makes it especially valuable for safeguarding cultural heritage, as it allows for continuous, large-scale monitoring without physical contact with the site, preserving both the integrity and the safety of historically significant areas.

By integrating InSAR data with TLS-based rockfall assessments, the study aims to correlate areas of high displacement rates

70 with actual rockfall occurrences. This comparison enhances the understanding of slope deformation dynamics, supports comprehensive hazard assessments for the area and presents the basis for rockfall modelling at certain areas of interest.

We applied RAMMS::ROCKFALL to evaluate hazard potential of small-scale cliff failures and calibrated friction parameters for RAMMS::DEBRISFLOW using historic, larger rock slope failures (e.g., the historic destruction of Thutmose III temple) that transitioned into granular flows as a reference.

75 Ambient vibration analyses have proven to be great assets for evaluating the development of preparing rock slope instabilities in alpine settings before eventual failure (Weber et al., 2018; Leinauer et al., 2024). For this reason, we integrated this promising technique in our approach and tested its applicability and data quality at this well-frequented heritage site.

This study is one of the first to transfer well-established methods from other mountainous regions into an integrated, non-invasive safeguarding approach for highly prestigious cultural heritage. Similar to the work in e. g., Petra, Jordan (Cesaro et

80 al., 2017; Margottini et al., 2017), we do not aim to push for technological advances rather than presenting a proof of concept of our approach in a challenging climatic, geomorphological and archaeologically sensitive environment. This multidisciplinary approach, integrating geological, archaeological and engineering perspectives, contributes to a comprehensive understanding of rockfall dynamics in the Theban Hills.

This paper ties to answer three questions: (i) How effectively can established non-destructive / non-invasive monitoring

85 techniques be integrated and transferred to priceless world heritage sites in challenging desert environments? (ii) To what extent can initial deformations in relatively young and not strongly cemented rocks be observed by LiDAR and InSAR? (iii) Can we derive potential runout scenarios and calibrate them with historical events, especially for fragmentation?

2. Study site

2.1. Temples of Deir El-Bahari

90 Dier El-Bahari Valley is situated in the West Bank 5 km from the Nile River in the Theban Mountains opposite Luxor city. Apart from Deir El-Bahari the area features some of the most renowned cultural heritage site of Egypt, such as the Valley of the Kings, Sheikh 'Abd El-Qurna or Dra Abu El-Naga. The complex of tombs and mortuary temples known as the Temples of Deir El-Bahari are dedicated to the many New Kingdom pharaohs over time. The Mortuary Temple of Hatshepsut, built in the 15th century BCE during the New Kingdom, is the main temple in this complex. It is a unique and well-preserved structure

95 that stands out for its architectural innovation and design. Designed by architect Senenmut, it features terraced levels, colonnades, and statues, dedicated to the sun god Amun-Ra, honouring Queen Hatshepsut's divine birth and pharaonic achievements (Ćwiek, 2014). Adjacent to Hatshepsut's temple, the Middle Kingdom's Temple of Mentuhotep II adds to the site's historical significance. The Temple of Thutmose III, wedged between the Temples of Hatshepsut and Mentuhotep II and carved partly into the rock, represents the New Kingdom era (Ćwiek, 2014).

100 Deir El-Bahari's cliffs boast tombs and chapels dedicated to various individuals, providing insight into the societal structure of ancient Egypt. This site is a testament to the cultural and artistic achievements of this civilization, encapsulating its historical depth and architectural prowess.
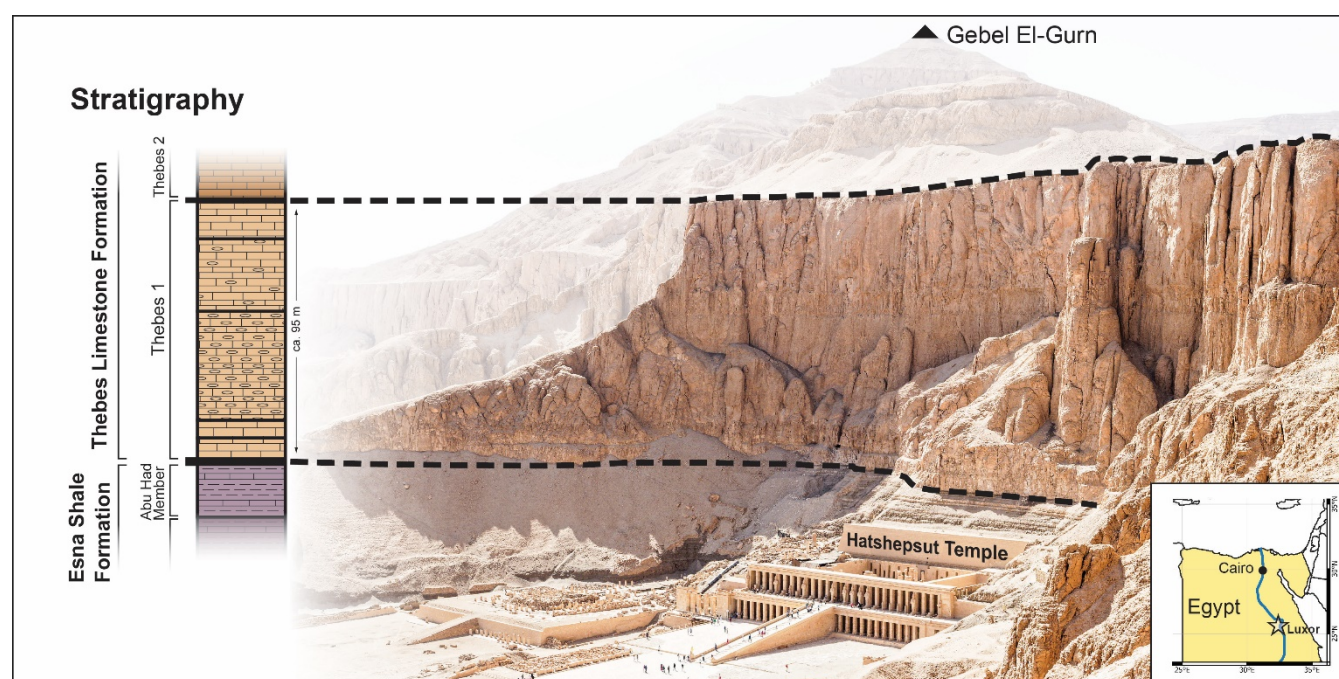
Figure 1: Topographic and geological setting of the Mortuary Temple of Hatshepsut within Deir el-Bahari. In terms of geo-
105 **mechanics, the relatively many-layered geological setup (Dupuis et al., 2011) can be reduced to a typical brittle on ductile structure.**

2.2. Geology

The terrain morphology of the study area resembles a Roman theatre-type shape, opening to the SE featuring a width of ca. 200 m and relief of ca. 140 m (Figure 1). Fluvial erosion and gravitational rock mass wasting processes, such as rockfalls or slides, were the main causes of the Valley's development in terms of morphology (Abdallah and Helal, 1990). Sub-horizontal
110 bedded rock members of Thebes Limestone Formation and Esna Shale Formation compose the cliffs of Deir El-Bahari (Said, 2017). The Esna shale Formation is a heterogeneous succession of shales that is usually subdivided into four members (Abu Had, El-Mahmiya, Dababiya Quarry and El Hanadi member) with a total thickness of > 60 m (Aubry et al., 2016). The top Abu Had Member, which is composed of an alternation of marl and limestone beds with a few clayey intervals, is increasingly carbonate-rich and has a sharp stratigraphic contact with the hanging Thebes Limestone Formation at the base of the cliff at

Deir El-Bahari (Aubry et al., 2009). The Thebes Limestone Formation described in detail by (King et al., 2017), who subdivides the Formation into five depositional sequences (Thebes 1-5) forming five typical cliffs in Thebes mountains (Figure 1, greyed out towards Gebel El-Gurn). Thebes 1, the lowermost unit with a thickness of ca. 90 m, forms the main rock face of the cliff at Deir El-Bahari, and is composed of thinly laminated pinkish marl, nodular micritic limestone and thinly bedded argillaceous limestones (Figure 1). Further stratigraphic subdivision is possible but not relevant for this study. Structurally, the lower Thebes Formation is a relatively soft and noticeably fractured limestone (Klemm and Klemm, 1993). In terms of geo-mechanics, the relatively many-layered geological setup (Dupuis et al., 2011) can be reduced to a typical brittle on ductile structure (Erismann and Abele, 2001).

Understanding and assessing the stability of the cliff above Deir El-Bahari requires an understanding of the geological structural framework as a crucial first step. Pawlikowski and Wasilewski (2004) mention two main structural features that affect the region are faults and fissures. Reactivation of most of these faults and fissures is attributed the Red Sea and Nile Valley tectonics during the Oligocene and Miocene. These tectonic activities have resulted in the normal (tensional) faults in Deir El-Bahri area, and the system of vertical fissures relates to them. The Thebes Limestone Formation is further dissected into several distinct rock towers (Figure 1) by vertical joints with dip angles ranging from 85° to 90°, striking N-S, E-W, NE-SW, and NW-SE (Hesthammer and Fossen, 1999; Pawlikowski and Wasilewski, 2004; Beshr et al., 2021).

2.3. Historic evidence of landslide activity

The geological and geomorphological characteristics of the cliffs of Deir El-Bahari valley indicate a long history of gravitational mass movement. According to the archaeological evidence, the temple of Thutmose III, neighbouring the Temple of Hatshepsut in Deir El-Bahari, was destroyed and superimposed by a major rock wall collapse (Lipinska, 1977; Arnold, 1996) which can be attributed to an earthquake around 1100–1080 B.C. (Karakhanyan et al., 2010).

Badawy et al. (2006) stated that six major earthquakes occurred in Middle Egypt during historical times, nearly destroying the Ramses III temple in Luxor on the west bank of the River Nile. (Abdallah and Helal, 1990) documented two rockfall events close to the Temple of Hatshepsut, one of which (ca. 20 m³) reached the upper court of the Temple of Hatshepsut in 1985. They emphasized the potential for rockfall events from the cliff and demonstrated the rock wall's susceptibility for failure at Deir El-Bahari.

Historical imagery from archaeological digs dating from the late 1890s over the 1930s to the 1970s show several geomorphological features, that could be attributed to gravitational mass movements (Naville, 1894; Winlock, 1942; Lipinska, 1977). However, major terrain alterations during these excavation campaigns induce extensive bias regarding geomorphological analyses. This is especially the case for the temple of Thutmose III which was only discovered in the 1960s and used as a sediment dump during other digs (Lipińska, 2007). We therefore only relied on the earliest image of the site from 1892 before the excavation (Figure 5) (Naville, 1894) to identify evidence of two probable historic gravitational mass movements (Sect. 3.3.2).

2.4. Definition of potential failure mechanisms

Judging from our review of literature, historic imagery and expert knowledge, we hypothesize two general potential failure types: (i) Single, locally constrained rockfalls ranging from ca. 0.01 to 25 m³ and (ii) the failure and collapse of larger
150 magnitudes, such as one of the distinct rock towers (Figure 1). Evidence of small rockfalls (< 0.15 m³) is shown in our multi-temporal TLS data and larger single events are documented by Abdallah and Helal (1990). The potential failure of a rock tower has been already postulated in the literature (Chudzik et al., 2022) and is obvious in historic photographs (Naville, 1894, 1907, 1913). Due to the in situ fragmentation of the heavily jointed rock mass and internal shear stress during the failure process, we expect the failing material to transition into a granular flow type behaviour, sometimes referred to as dry flow (Hungr et al.,
155 2014).

3. Methods

3.1. Terrestrial Laser Scanning

We deployed a Riegl VZ-400 terrestrial laser scanner to obtain multi-temporal high resolution topographic data and to perform a rock surface change detection. In late February 2022 TLS data was gathered at six locations around the Temple of Hatshepsut.
160 In early March 2023, we repeated the scans at the previous positions and added ten additional scan positions to increase data coverage on top of the Deir El-Bahari cliff (Figure 2). We used RiScan Pro for all raw data processing (filters, registration (MSA), geo-referencing). The data sets of both scan epochs were each merged, homogenized and trimmed to single 3D point clouds of Hatshepsut's Temple and the cliff behind. To generate a detailed digital surface model (DSM), the point cloud of 03/2023 was manually edited in the open-source software CloudCompare to exclude tourists and optimize geomorphometric
165 accuracy in the inner temple area (occluded flooring, roof structures and pillars) before the final 2.5 D rasterization. We applied linear interpolation for small, inevitable data gaps. We used the standard Multiscale Model to Model Cloud Comparison (M3C2) algorithm by Lague et al. (2013) to perform a straightforward topographic change detection, which we limited to the rock face, scree slopes and retention wall behind the temples of Deir El-Bahari. For the visualization of our data we worked with Cloud Compare and QGIS.

170 ### 3.2. Interferometric Synthetic Aperture Radar

This study employs Interferometric Synthetic Aperture Radar (InSAR) data from Sentinel-1 satellites to monitor ground displacements at the Mortuary Temple of Hatshepsut. The Area of Interest (AOI) was covered exclusively by the only available ascending (ASC) geometry, which aligns well with the site's topography, reducing layover and foreshortening effects, and is well-suited for observing mass movement processes on the east-exposed slopes.
175 The InSAR analysis was based on a time series of Sentinel-1 ASC data collected between January 5, 2021, and February 19, 2024. A total of 93 radar datasets were processed using the Persistent Scatterer InSAR (PS-InSAR) algorithm implemented in

PYGMTSAR (Pechnikov, 2024). This approach identifies stable radar targets, known as persistent scatterers, to detect displacements along the Line of Sight (LOS) with high precision.

The primary objective of the InSAR analysis is to identify areas with higher yearly displacement rates and compare them with
180 areas of documented rockfall activity assessed using TLS. We analysed the spatial distribution of yearly displacement rates to highlight recent changes in ground stability, making it easier to identify active zones. This approach provides more timely insights for assessing rockfall risks compared to cumulative displacement maps, which only show total movement without reflecting current activity levels.
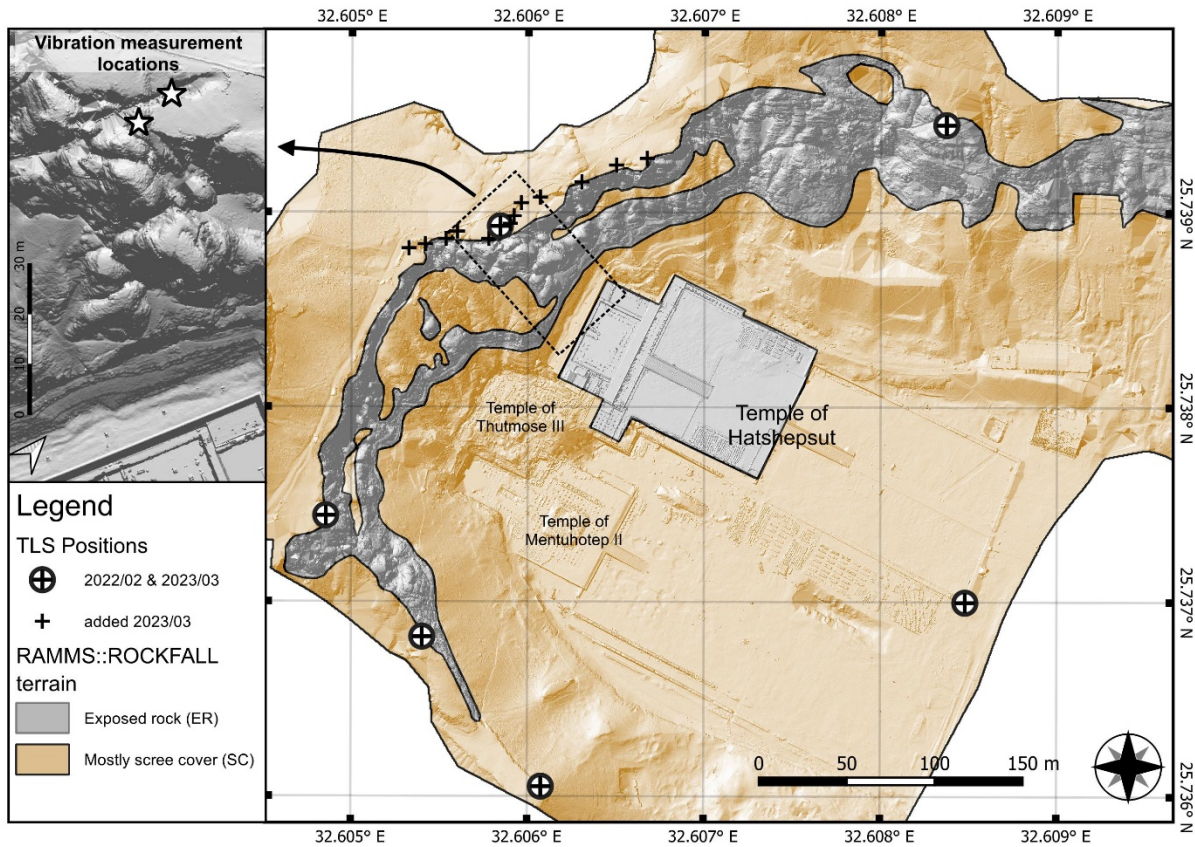
185 **Figure 2: Locations of TLS Positions, vibration measurements, and spatial extent of terrain for RAMMS::ROCKFALL simulations.**

3.3. Runout Modelling

In this study we used the RAMMS-Software suite (RApid Mass Movement) to simulate runout scenarios for the two main failure mechanisms hypothesized for the rock wall at Deir EL-Bahari (Sect. 2.4) to produce a first benchmark towards a
190 comprehensive risk analysis. We used RAMMS::ROCKFALL for the simulation of single, locally constrained rockfalls ranging from ca. 0.01 to 25 m³ and RAMMS::DEBRISFLOW for granular flow parameterization of two probable historic,

larger collapsed rock towers. As our monitoring data does not show any imminent larger rock wall failure, the granular flow simulation retained in a parameterization stage, focused on historic events. We used the RAMMS-software suite as it allows a comprehensive and intuitive modelling approach and straightforward parameterization.

3.3.1.   Rockfall simulation

RAMMS::ROCKFALL is a numerical simulation tool that models rockfall trajectories, velocities, and impact forces using non-smooth rigid body mechanics coupled with hard contact laws. It integrates digital elevation models and material properties to assess hazard zones, optimize mitigation strategies, and support risk analysis in complex terrain (Caviezel et al., 2019). We set up RAMMS::ROCKFALL models for three potential release areas, that we identified from the TLS and InSAR integration (Figure 3c), which we labelled A01, base of the Thebes Formation behind the Temple of Hatshepsut, A02, rock tower above the Temple of Hatshepsut, and A02, rock face at western Deir El-Bahari. For each release area we created four rockfall scenarios referring to the released block sizes of 0.01, 0.1, 2 and 25 m³. We attributed these magnitudes to theoretical return periods (frequency) of 5, 1, 0.05 and 0.01 a^{-1}, respectively. This magnitude frequency relation corresponds roughly to a power law ($F(V) = 1.2V^{-0.82}$), which fits well in the range of other rockfall studies (Graber and Santi, 2022).

Key parameters for rockfall dynamics are rock shape and the terrain parameters (Caviezel et al., 2019; Caviezel et al., 2021). To obtain applicable rock shapes we gauged (i) the general shape of the occurred rockfalls in the TLS change detection and (ii) multiple larger blocks in or at the base of the cliff using our 3D point cloud (S1, S2). This resulted in rock aspect ratios of ca. 1 / 0.6 / 0.5 which refers to a "long" rock shape with rounded edges in RAMMS' Rock Builder. We estimated terrain parameters according to RAMMS AG (2024b) and chose "hard" for the scree slopes and "extra hard" for all solid rock surfaces (cliff and temple floor, Figure 2). As suggested, we increased the ground dampening of the scree slopes slightly for the largest rock volumes (RAMMS AG, 2024b). With these rather high terrain categories we aim to produce a conservative first estimate of potential runout lengths. We used a 0.5 m grid resolution, and 20 random start orientations at every sixth grid point for all simulations. Please refer to S3 for a full list of parameters.

3.3.2.   Granular flow simulation

As stated in 2.4, we expect a potentially failing and collapsing rock tower to transition into a granular flow type behaviour. To determine suitable parameters for potential granular flow events at the Temple of Hatshepsut, we calibrated two RAMMS::DEBRISFLOW scenarios. The model is based on the shallow water equations with a two-parameter rheology that accounts for both frictional and viscous flow properties (dry-Coulomb type friction μ and viscous-turbulent friction ξ). It allows users to predict flow paths, velocities, impact forces, and deposition patterns using high-resolution digital elevation models (DEMs) (RAMMS AG, 2024a). RAMMS::DEBRISFLOW is widely applied in hazard assessment, risk management, and mitigation planning for debris flow-prone areas.

The oldest available photograph of the Temple of Hatshepsut from 1892 (Naville, 1894), shows two likely granular flow deposits of collapsed rock towers: Event A (ca. 5000 m³ or 100 m²*50 m height) behind the temple of Thutmose III and event

B (ca. 2600 m³ or 52 m²*50 m) north of the Temple of Hatshepsut (Figure 5a). We estimated release volumes from historic imagery, the 3D point cloud and simple geometric and morphometric assumptions of geomorphological features (S4) and archaeological reports of cliff cleaning missions (Zachert, 2014a, 2014b, 2014c). As these missions removed most of the scree on the slope area of event A, we assume to have obtained pre-failure slope coverage in our laser scans. To achieve the same for event B, the recent talus cone north of the Temple of Hatshepsut was removed and interpolated in the DSM. Start locations for events A and B were determined by a GIS-based flow path analysis and geomorphological study of the rock wall. For simplicity, we assume that for both model scenarios all material identified as possible historic rock slope failure was released at once using a five second hydrograph and an initial velocity of 15 m/s in the down slope direction. The initial velocity was estimated with a mean maximal vertical velocity of the collapsing mass of 20 m/s and coefficient of restitution considerations presented by Jackson et al. (2010). We calibrated the granular flow models for events A and B by varying both friction parameters between $0.4 < \mu < 0.8$ and $500 < \xi < 5000$ m/s² and comparing the model results to the respective post-failure geomorphology (height and run out pattern of deposits). Please refer to S5 for a full list of parameters.

3.4. Vibration measurements

In the scope of preliminary field tests, seismic measurements are recorded to determine which vibrational quantities are suitable precursors for sudden or gradual material changes in the rock needles behind the Temple of Hatshepsut. The considered methods include horizontal-to-vertical spectral ratios (HVSR), standard spectral ratios based on ambient noise (SSR), and the stochastic subspace identification (SSI). One sensor is placed at the top of the rock needle and another is located in the gap between the rock needle and the plateau (Fig. 2).

The horizontal-to-vertical spectral ratio (HVSR) is a common tool to analyse the amplification of ground motions on site based on a single tri-axial sensor (Nakamura, 1989). Resonance frequencies can be extracted from HVSR curves as the x-value of predominant peaks (Figure 6). The standard spectral ratio (SSR) is another concept to describe the site amplification. It is defined as the earthquake spectrum of a reference site in comparison to the examined site. Therefore, SSR requires at least two uni-axial sensors, where one of them must be located on bedrock. A SSR beyond one describes the site amplification, and the peaks represent resonance frequencies. The stochastic subspace identification (SSI) is an appropriate method to determine modal parameters of a structure (van Overschee and Moor, 1995). SSI can be performed based on a single measurement channel. The method yields the natural frequency f_i and damping ratio ζ_i of each mode of vibration i. The algorithm requires the number of modes m to be set as a user input. Since this value is unknown a priori, the computation is repeated for a user-defined range of modes, and the model order of each solution is plotted against the frequencies in so-called stabilization diagrams, see (Figure 6). A detailed technical description of the data analysis is provided by Mendler et al. (2024). All three methods yield resonance frequencies of the soil and this paper sets out to compare their effectiveness and robustness for exposed rock needles, such as the one behind the Hatshepsut temple.

4.   Results

4.1. Terrestrial Laser Scanning

The finished point clouds of our TLS campaigns show an almost full coverage of the Deir El-Bahari area, including temples, the cliff and the geometry of the most prominent rock pillars behind the Temple of Hatshepsut, including fissures running behind them. Both point cloud models have X, Y, and Z dimension of ca. 1000*650*200 m, contain ca. 85 Mio. points with a point-to-point distance of 0.05 m. The registration error for the first epoch (02/2022) was just over 0.01 m (standard deviation of residuals) whereas it was ca. 0.03 m for the second epoch (03/2023). The data of the latter was rasterized to DSMs with raster sizes of 0.1, 0.5 and 1 m for the purpose of runout modelling and data visualization.

Figure 3a shows the results of the surface change detection. For better visual accessibility, we subsampled the change detection to a point spacing of 0.25 m and 100 significantly changed points in a radius of 1 m. The original change detection is shown in Figure 3a (right side). Generally, the data does not reveal extensive rock face deformation above the level of detection (LoD) of 0.03 m. Hence, no larger imminent mass movements were detected. At the base of the Thebes Formation five distinct small rockfalls source areas with magnitudes from 0.05 to 0.15 m³ occurred behind the Temple of Hatshepsut between the scan epochs, where one event most likely occurred as three smaller rockfalls. The deposits of these rockfalls are also detectable and are situated either outside the temple area or behind the retaining wall protecting the temple (Figure 3a, right side). For an area of ca. 6,5 ha of exposed rock wall (S6), we calculated a total rockfall volume of 0.589 m³, which translates to a rock wall retreat rate of ~0.009 mm/a. Minor sediment redistribution, recognizable by typical erosion and deposition patterns, is mostly restricted to the scree slopes, small gullies, and an area around a rock tower and its base north of the Temple of Hatshepsut. The data also show enhanced terrain alteration at an ongoing archaeological dig site behind the temples of Thutmose III and Mentuhotep II, neighbouring the Temple of Hatshepsut. These data are not shown in this study, but their location is disclosed in Figure 3b.

4.2. Interferometric Synthetic Aperture Radar

All available satellite tracks from the Sentinel-1 (SNT) mission were processed to generate a comprehensive InSAR dataset. The temporal distribution of the acquisitions is shown in Table 1 and S7. Over the full observation period, more than 19,000 measurement points were identified in one km², with an average standard deviation of 2.7 mm/a for the estimated displacement velocities (Table 1).

Table 1: Used InSAR datasets, number of measurement points (MP), MP density and standard deviation of the analysed InSAR data sets.

Satellite	Geometry	Satellite track	Look dir. φ [° N]	Incidence angle β [°]	# Images	Acquisition period	MP [#]	Ø St. Dev. [mm/a]
SNT	ASC	T58	80	40	88	05.01.2022-19.02.2024	19,419	2,7

285

The processed InSAR data reveal deformation velocities of up to 30 mm/a in the immediate vicinity of the temple complexes (Figure 3.b). Due to the C-band wavelength of Sentinel-1 and the applied processing method, each measurement point integrates surface motion over an area of approximately 60 m² (pixel resolution: 4 × 15 m). By integrating three years of satellite data and applying time series curve fitting, line-of-sight (LOS) velocities were derived for each persistent scatterer.

290 Based on the statistical characteristics of the dataset, velocities exceeding ±5 mm/a are considered significant (see Table 1). To contextualize the spatial patterns, the study area was subdivided into exposed rock (i.e., the cliff) and adjacent scree deposits. The analysis yields four key observations: (i) Widespread stability – The majority of the terrain, including most parts of the rock face surrounding the temples, does not exhibit significant displacement. (ii) Localized rock face activity – Significant velocities within the cliff area are restricted to small zones, specifically, at the base of the cliff, a rock tower north

295 of the Temple of Hatshepsut, and a slope area west of the Temple of Mentuhotep II (S8). (iii) Data gaps – Central parts of the site show sparse or missing data, mainly due to radar shadowing from steep terrain or phase decorrelation, potentially linked to archaeological excavations. (iv) Activity in scree deposits – The most pronounced and spatially extensive deformation is observed in the scree southeast of the Temple of Mentuhotep II, suggesting increased susceptibility to surface movement in these unconsolidated materials.

300 **4.3. Identification of areas of interest**

The combination of TLS and InSAR analyses allow for joint interpretation and the definition of areas of interest (AOI). In the area behind the Temple of Hatshepsut both the TLS and InSAR measurements result in similar patterns: several small rockfalls, scree redistribution and aeras with statistically significant InSAR velocities are evident at the base of the cliff. Furthermore, there are patches of negative surface changes just above the LoD (0.03 m) around and below a distinct rock tower north of the

305 temple, and statistically significant ground movement towards the radar sensor are in the same spot. These two regions of potential rockfall activity are defined as release areas A 01 (base of the cliff) and A 02 (rock tower) for the rockfall runout activity. We further suggest that, based on our results, the area behind the Temple of Hatshepsut has an increased monitoring demand (Figure 3c). The same is true for a patch of rock wall in the western part of Deir El-Bahari, defined as rockfall release area A 03 (Figure 3c, left; Figure). Here, the InSAR results show statistically significant ground movement that is below the

310 TLS threshold.
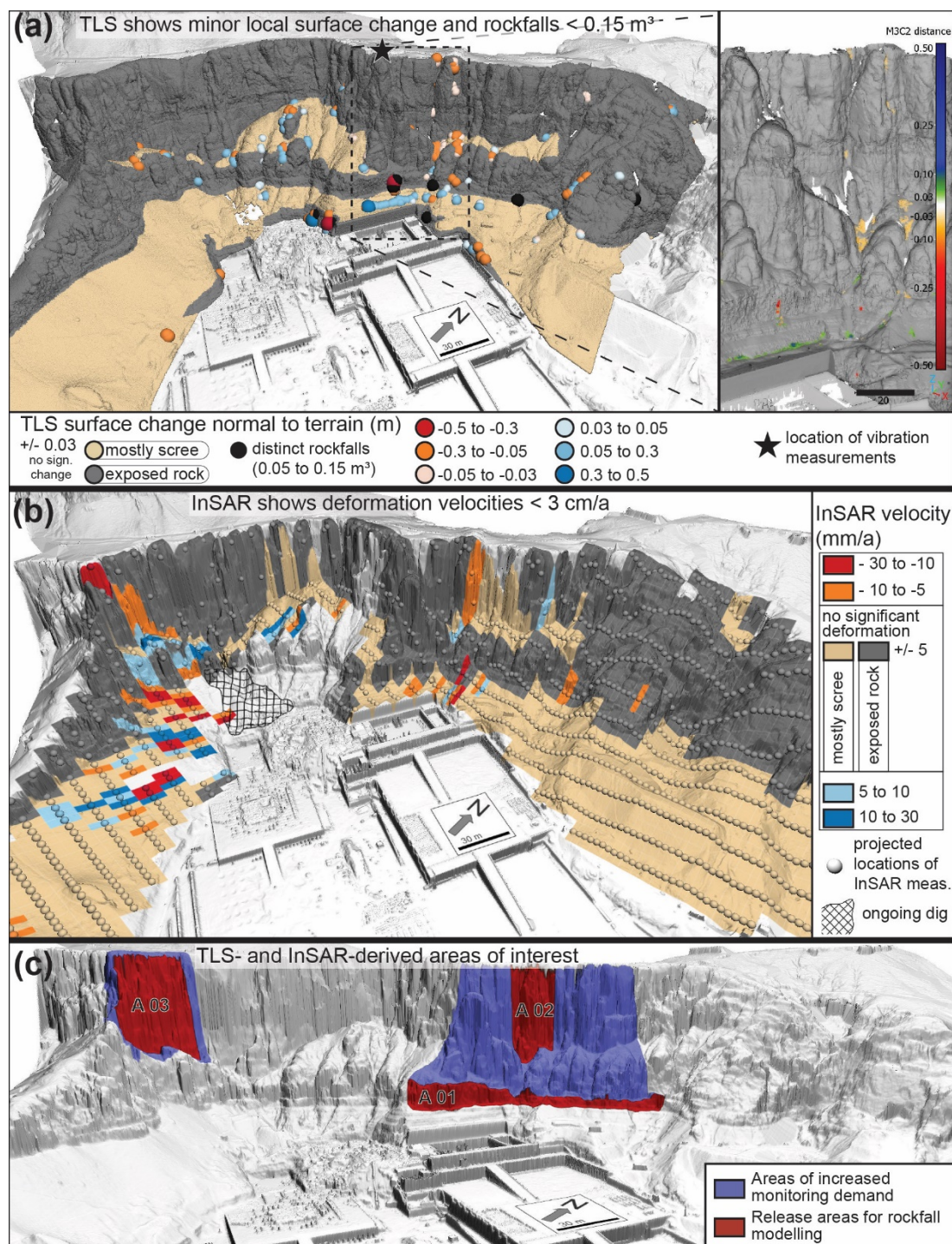
Figure 3: a) TLS change detection 2022/02 – 2023/03. Significantly changed areas. Detailed view of changes in point cloud in the top right panel. Changes due to digging and anthropogenic terrain alterations were removed. B) InSAR velocities, trend over three-year period, filtered by ground cover (mostly scree covered / exposed rock surface). c) TLS- and InSAR-derived areas of interest.

4.4. Runout Modelling

4.4.1.   Rockfall simulation

Figure shows the results of the rockfall runout modelling. We chose to depict the total reach probability of released rocks per
scenario to highlight (i) maximum runout lengths and (ii) probable travel paths at each AOI. A total of 93,600 simulations
were performed to produce statistically sound results. The Figure illustrates that rocks from release scenarios A 01 and A 02
have a certain probability (3.8-18.1 %) of reaching the accessible area of the Temple of Hatshepsut while rocks from scenario
A 03 do not reach it in the model. The rocks from A 03, however, do reach the ancient temples of Mentuhotep II and Thutmose
III, which are not accessible to the public. Rocks from scenario A 01 (base layer of Theben Formation) generally have a lower
probability of reaching the temple than scenario A 02 (rock tower above the Temple of Hatshepsut) and are mostly deposited
on the retention wall behind the Temple. The number of rocks deposited in the Temple of Hatshepsut visitor perimeter is
proportional to the magnitude of the released rocks, i.e. larger rocks have a longer runout. However, the difference between
the smallest (0.01 m³) and largest rocks (25 m³) is rather low, with total reach probabilities ranging from 3.8 to 13.6 % for
scenario A 01 and from 12.3 to 16.1 % for scenario A 02.
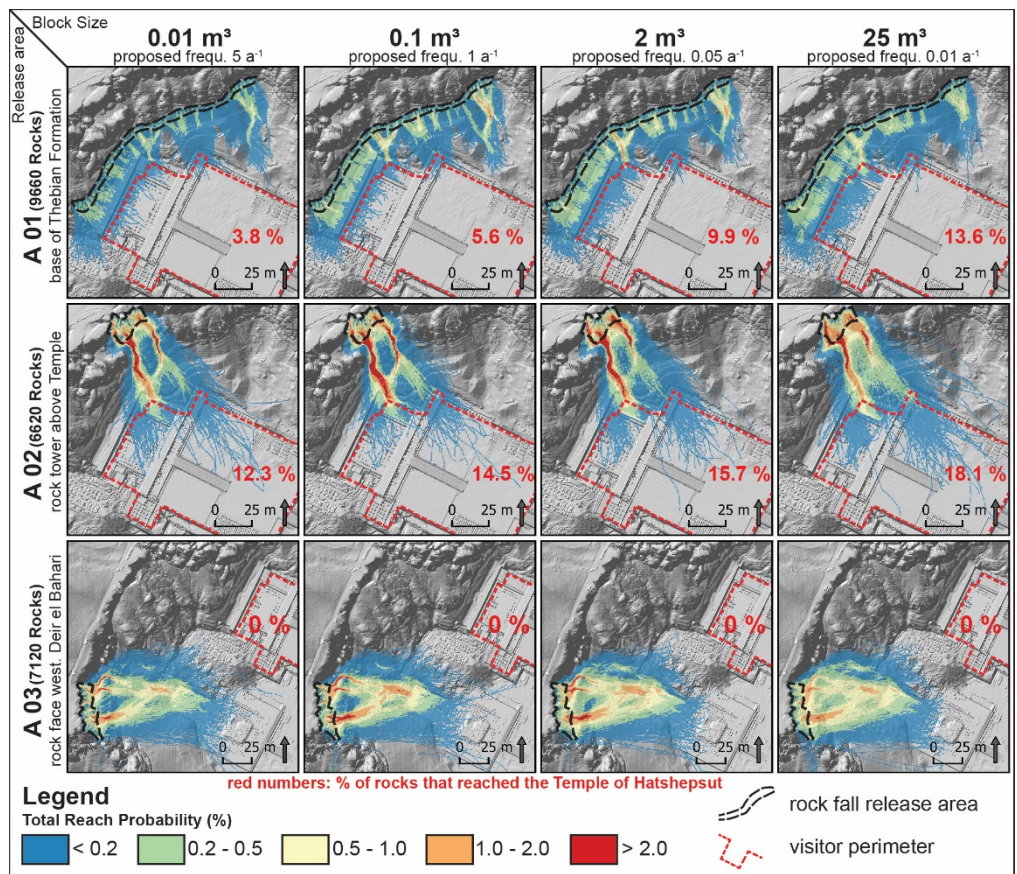
Figure 4: Results of the rock fall simulations for scenarios A 01 (base of Theben Formation), A 02 (rock tower above the Temple of Hatshepsut), A 03 (rock face west of the temples), and different rock sizes.

4.4.2. Granular flow simulation

Figure 1a shows the two historic slope failure deposits we identified for our subsequent model parameterization. Both deposits exhibit (i) typical cone shape geometry, (ii) an intermixture of large rock fragments that indicate remnants of the collapsed rock tower, and (iii) at event A a comparatively thick scree cover with boulders on the slope above the furthest deposits.

335 Figure 5b and c show the results the simulation results (deposition height) for the overall best fitting internal friction parameters of $\mu = 0{,}65$ und $\xi = 800$ m/s². The height and spatial distribution of the simulated deposits show a good fit to the geomorphological condition prior to the excavations at the Temple of Hatshepsut. Simulations of event A show (i) major deposits in the Thutmose III temple perimeter, that would have caused considerable damage to the former structure, and (ii) relatively extensive deposits on the slope. Event B shows a wide, cone-shaped deposit in the simulation and some spill in 340 today's reconstructed temple complex. Of course, the event would have happened long before reconstruction, therefore, unequivocal validation of the runout remains a challenge.
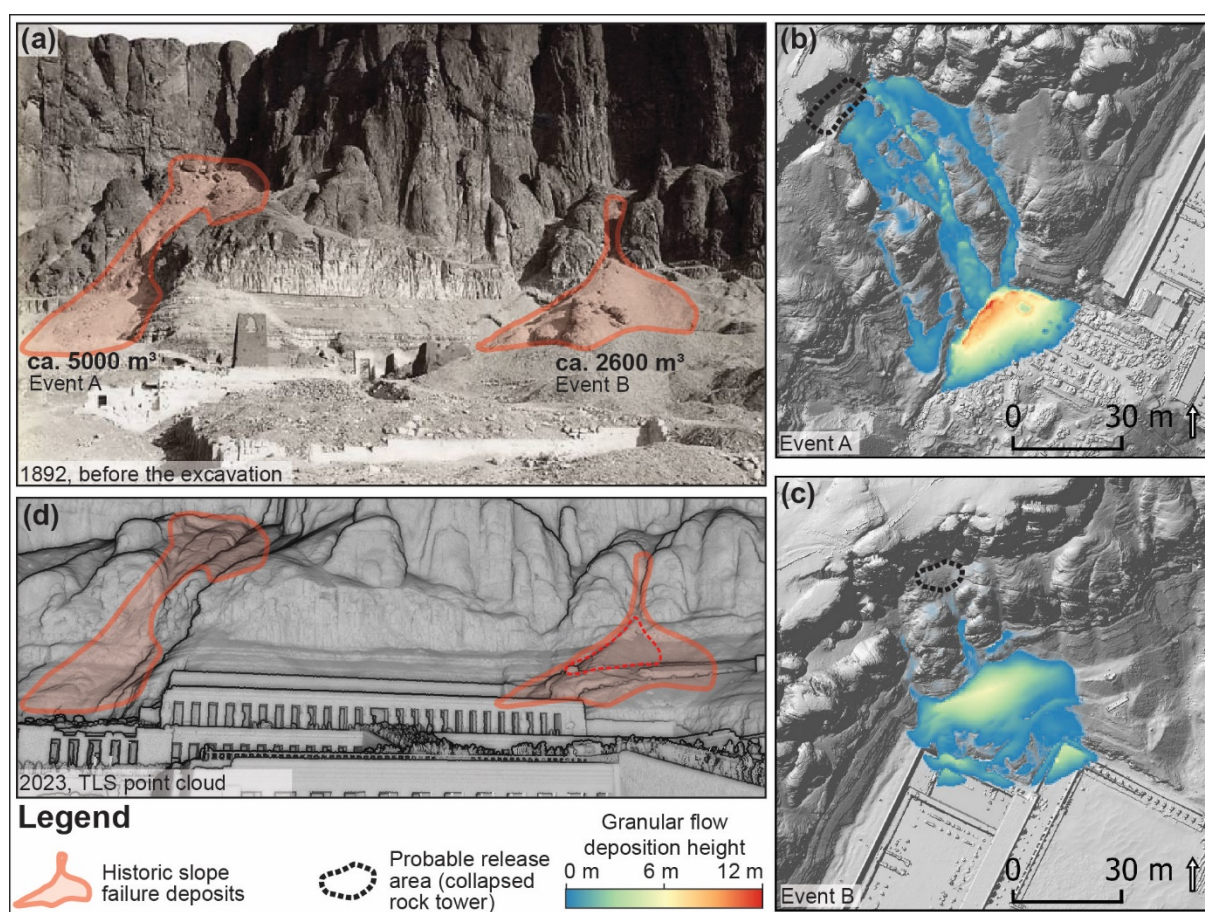
Figure 5: a) Earliest historic photograph of the Temple of Hatshepsut before major excavation (Naville, 1894) shows two distinct deposits that are most likely linked to previous rock slope failure. b), c) Results of the dry flow simulations for historic rock tower 345 **collapse and subsequent granular flow. D) current 3D TLS point cloud; the recent talus cone, marked by the red dashed line, was removed from the model before the simulations.**

4.5. Vibration measurements

The results of the vibration monitoring are summarized in Figure 6, which displays representative HVSR, SSR spectra and a SSI stabilizing diagram, and the permanent tracking of the extracted frequencies. The uncertainty in the measurements is
350   quantified through the 65% confidence intervals for HVSR and SSR curves (light red), and error bars equivalent to the 65 % confidence interval for the SSI.

The extracted frequencies are similar for all methods, with values of about 13, 34, 56, and 67 Hz. The SSI method appears to be most suited for long-term monitoring, as it is the only method that can continuously identify all four modes of vibration, even the weakly excited mode around 34 Hz which does not lead to a peak in the power spectral density (Figure 6 bottom).
355   The most dominant mode around 56 Hz is reliably identified by all three methods. Where HVSR fails to reliably identify the other modes, SSR appears more suitable for the estimation of high-frequency modes, such as the one around 67 Hz.
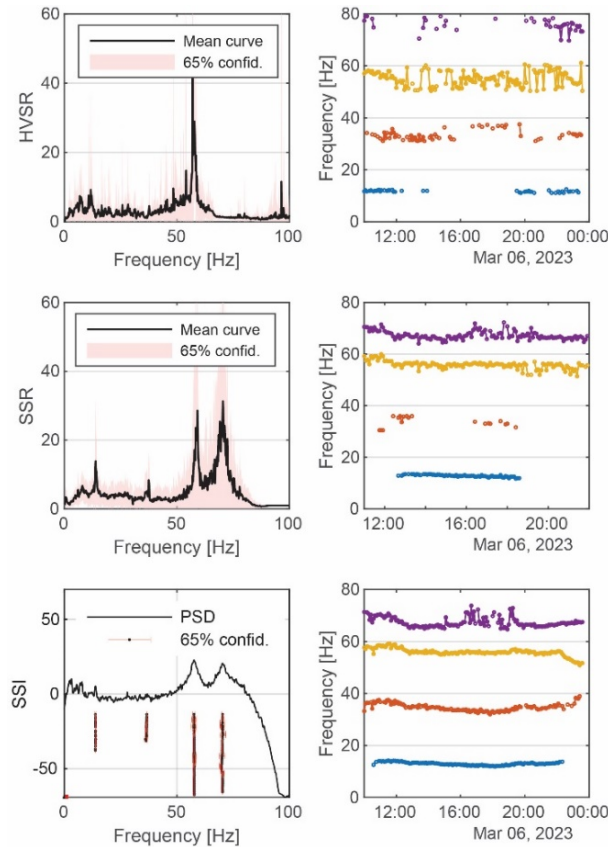
Figure 6: Extracted frequencies based on HVSR, SSR, and SSI.

360   Every method has a unique selling point. The SSI method is the only method that yields (undamped) natural frequencies f_i and damping ratios in percent critical damping ζ_i. It is also the only method that does not depend on the user-defined frequency resolution. Although not shown here, SSI can also be used to estimate mode shapes. Modes shapes characterize the deflection

pattern and the directivity of each mode of vibration, giving deeper insights into the most likely stress accumulations and failure scenarios. HVSR and SSR, on the other hand, give information on the spectral site amplification of ground motions.

365   Sudden changes in frequencies or damping ratios can be indicators of material changes in the rock; however, vibrational modes also oscillate due to environmental effects, such as material temperature and moisture content. In this preliminary study, the compounding effects are not measured, but Figure 7 shows the SSI-based natural frequency and damping ratios, together with the ambient temperature and wind speed measured at a nearby weather station in Luxor. The damping ratio shows the most distinct changes ranging from 1% to 4.2%. On close inspection, the correlation between the variables becomes obvious:

370   increasing ambient temperatures lead to decreasing frequencies and higher damping ratios. The correlation becomes more obvious when a time lag of a few hours is considered, as vibration behaviour depends on the material temperature and not the ambient temperature. Further technical insights and results are addressed in Mendler et al. (2024).
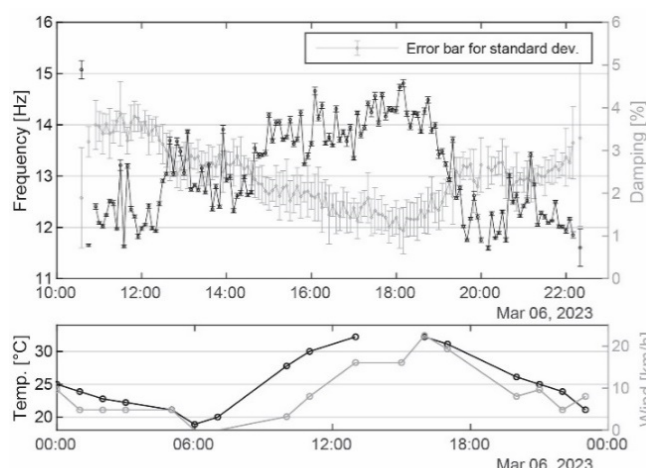
Figure 7: Environmental factors that influence *natural* frequencies and damping ratios.

375 **5. Discussion**

5.1. Terrestrial Laser Scanning

The TLS surveys produced vital data for DSM generation – the basing for all runout simulations and topographic analyses – and surface change detection. The level of detection (LoD) of 3 cm is in the range or below comparable topographies (Santos Delgado et al., 2009; Abellán et al., 2010; Jacobs and Krautblatter, 2017; Mohadjer et al., 2020). The LoD is the instrumental

380   error, controlled by the error propagation from raw data quality and registration process. In our analysis the LoD is produced as significant change calculated by the M3C2 algorithm (Lague et al., 2013), and also corresponds to the 95th percentile of model distances (similar to Abellán et al. (2011)). Our data show that environmental condition at Egyptian heritage sites have major impact on data quality and thus LoD. Relative humidity is generally very low which positively affects accuracy (alignment std. dev. 0.01 m for 02/2022 data), but desert dust and drastic diurnal atmospheric temperature variations can have

385 the opposite effect (Witte and Schmidt, 2006). This became an issue for the second TLS campaign (03/2023), where extensive filtering in some point clouds was needed to reduce residual distances to 0.03 m.

Despite the high degree of rock mass fragmentation, compared to other TLS-based rockfall studies, the calculated retreat rate, and hence the rockfall activity, is very low (Abellán et al., 2010; Jacobs and Krautblatter, 2017; Strunden et al., 2015; Draebing et al., 2024). We attribute this to a lack of climatic controls (e.g., rain, moisture, freezing) that are limited to thermal erosion

390 (Collins and Stock, 2016) and seismic acceleration. However, we stress that in a rare case of significant precipitation event a stark increase in rockfall activity is highly probable (Krautblatter and Moser, 2009). This is particularly important as regional precipitation patterns in Egypt are expected to change due to global climate change (Gado et al., 2022).

All few detected distinct rockfalls are restricted to the very base of the cliff, which we attribute to increased topographic stress. Over long time scales this erosion pattern can lead to oversteepening, reducing the cliff's toe support (Rosser et al., 2013) and

395 promoting larger instabilities. Scree redistribution pattern in the TLS change detection on the talus slopes (Figure 3a) are either linked to small trails or small gullies in the rock mass where minor disturbances (workers or very small rockfalls) can result in small granular flows in the scree deposited at its angle of repose.

This study shows that TLS in the context of safeguarding cultural heritage in hyper-arid regions is very well suited for high-resolution surface change / rockfall detection. Rapid change of local atmospheric conditions (e.g., temperature, dust) may

400 reduce data quality on a short-term basis. Other studies have shown that TLS is well-suited for detecting larger slope instabilities even before eventual failure (Santos Delgado et al., 2009; Jacobs et al., 2024; Kenner et al., 2022). Depending on future safety demand, we aim to extent the multi-temporal TLS data set to (i) increase our understanding of rockfall dynamics at the Temple of Hatshepsut, (ii) potentially detect larger instabilities prior to failure or (iii) integrate a TLS system in a 4D early warning system (Gaisecker and Czerwonka-Schröder, 2023; Winiwarter et al., 2023).

405 **5.2. Interferometric Synthetic Aperture Radar**

The InSAR-based analysis of ground deformation around the temple complexes of Deir El-Bahari reveals a spatially heterogeneous pattern of ground movement, with most of the study area showing stable conditions over the three-year observation period. Crucially, the exposed rock face, including the immediate surroundings of the temples, appears largely stable, supporting the assumption of relative geological inactivity in these zones. This finding is particularly relevant given the

410 cultural and historical value of the area, providing a quantitative baseline for conservation and risk management.

A key strength of this study is the exceptionally high quality of the InSAR data. This is largely attributable to the favourable environmental conditions of the study site: the arid desert environment offers minimal vegetation cover, low surface moisture, and relatively stable atmospheric conditions. These factors significantly reduce decorrelation and atmospheric noise – two of the main challenges in InSAR processing – resulting in dense and reliable measurement coverage across the terrain.

415 Localized zones of significant displacement were identified at the base of the cliff, around a rock tower north of the Temple of Hatshepsut, and above the Temple of Mentuhotep II. These zones may reflect small-scale rock mass instabilities that require further investigation. The scree southeast of the Temple of Mentuhotep shows notable movement, likely linked to gravitational

reworking or human activity. Data gaps in central areas are primarily attributed to radar shadowing due to steep terrain or phase decorrelation, potentially caused by archaeological activities. Despite these limitations, the overall measurement density and precision offer a robust foundation for long-term monitoring.

In sum, this study underscores the value of multi-year Sentinel-1 InSAR monitoring in hyper-arid, topographically complex environments. It not only enables detailed mapping of ground stability but also supports the identification of localized hazards – an essential step in the sustainable management of vulnerable heritage sites.

5.3. Runout Modelling

5.3.1.   Rockfall simulations

The results of the rockfall runout simulations are mostly dependent on rock shape and the terrain parameters (Caviezel et al., 2019; Caviezel et al., 2021; RAMMS AG, 2024b). We chose a "long" rock shape with an aspect ratio of ca. 1*0.6*0.5, as this proved to be the best fit for the Site (see Sect. 3.3.1). Principally, other rock shapes cannot be ruled out entirely and should be addressed in future in depth analyses. The terrain parameters in our model are relatively simple and hard, compared to other studies from mountainous areas (Noël et al., 2023; Massaro et al., 2024), but serve as a conservative estimate and are consistent with RAMMS AG (2024b) as examples from entire unvegetated environments are scare. Calibrating terrain parameters with rockfall remnants on site is heavily biased as the entire plain of Deir El-Bahari has been dug out and cleaned from debris. Therefore, existing rockfall deposits outside the temple perimeter may represent statistical outliers rather than reliable calibration events.

The results show less influence of rockfall magnitudes on runout length than anticipated. This is, however, consistent with Caviezel et al. (2021) and can, in this case, also be attributed to the large vertical component of the trajectory and the high DSM surface roughness in the archaeological sites (especially Scenario A 03, temple of Mentuhotep), as RAMMS::ROCKFALL does not allow plastic deformation of the surface model – in this case archaeological structures. The results of our TLS-based rockfall detection show that all detected rockfalls intensely fragment upon their deposition, resulting in energy dissipation. As our simulations cannot account for fragmentation during the rockfall trajectory, we probably overestimate total reach probabilities to some extent. Here, is important to note that reach probabilities do not include incident probabilities which are key for future work towards risk assessment. In summary, our rockfall runout simulation offers a first, straightforward and conservative approach towards rockfall hazard assessment at the Temple of Hatshepsut.

5.3.2.   Granular flow simulations

As rockfalls in the geological context of Deir El-Bahari exhibit a large susceptibility to fragmentation, the granular flow simulations produced valuable insights into potential runout scenarios, especially for larger magnitudes. RAMMS::DEBRISFLOW was originally developed for the simulation of debris flows and its application in completely dry environments may seem counterintuitive. However, it turned out to be a simple and geomorphologically accurate simulation

tool for dry flows (granular flow), too. The model calibration produced comparatively high values for the dry-Coulomb type
450   friction μ, as there is no lubrication effect of water (RAMMS AG, 2024a). The runout and height of the deposits are mainly
controlled by μ, whereas viscous-turbulent friction ξ controls velocity and the amount of material, deposited on the slope.
Since information on release volumes is limited to single historic photographs, anthropogenic terrain alterations are massive,
and our remote sensing data do not suggest distinct imminent unstable volumes, the simulated granular flow magnitudes are
rough geometric estimates and assume spontaneous rather than successive failure. They translate to rock towers with a height
455   of ca. 40-50 m and a footprint of 65-100 m², which is very similar to other rock towers structures at the Deir El-Bahari cliff.
Therefore, our simulation provides key parameters for the simulation of potential future events.

5.4. Vibration measurements

This paper demonstrated the advantages of the SSI method for vibration monitoring. It is the only method that estimated all
modes of vibration with high accuracy and a short measurement duration (of 5 min). Unusual weather events may lead to
460   erosion and cracks within the material, reduced compound stiffness, and hence, irregular changes in the frequency and damping
values. Therefore, vibration-based features can be suitable precursors for rockfalls and could be employed to inform authorities
and give them the opportunity to initiate on-site investigations, or to rerun the TLS and InSAR analyses on demand.
The study highlights that environmental changes affect the vibrational behaviour of the examined rock tower. Damping ratios
appeared to be particularly susceptible to changes in environmental factors, and consequently, material changes (Figure 7). To
465   be able to distinguish normal changes from structural damage, the seismic station must be equipped with sensors that measure
environmental variables that influence the vibration behaviour of the rock tower. Moreover, measurement data from an entire
seasonable cycle (one year), or better two, needs to be measured to train smart algorithms to detect anomalies and quantify
long-term shifts.

5.5. Discussion of safeguarding and hazard anticipation strategy

470   The combined analysis of the TLS and InSAR data congruently reveals largely stable conditions at the cliffs of Deir El-Bahari.
Most detected surface change is confined to the scree slopes of archaeological activity. This finding holds particular
significance due to the area's cultural and historical importance, offering a quantitative basis for conservation efforts and a
benchmark for future risk management. One of the main strengths of this study is the exceptionally high quality of the remote
sensing data, which can be largely attributed to the favourable environmental conditions at the study site. Two localised zones
475   of significant activity were independently detected by TLS and InSAR, one by InSAR only, underlining their complementary
capabilities. This is even more notable when looking at spatio-temporal scales of our monitoring approach. InSAR can cover
vast amounts of area with very high accuracy (mm), but low spatial resolution. TLS offers the highest spatial resolution, good
accuracy (3 cm LoD), but less coverage when the short measuring intervals are demanded. The measuring interval and
processing time can be prospectively optimized by using automated approaches (Williams et al., 2018; Winiwarter et al., 2023).
480   By successfully showcasing the applicability and potential of continuous ambient vibration measurements at the site, we offer

a way to close the scale gap between InSAR and TLS. Abrupt rock mechanical changes in local, potentially instable zones could be detected instantaneously by a change in frequency spectra, even if they are below TLS LoD or between InSAR satellite passes.

The integrated rock face deformation data yields three local zones of potentially active gravitational mass movements: the cliff
485 base behind the Temple of Hatshepsut, a rock tower north of the Temple of Hatshepsut and a patch of rock face behind the Temple of Mentuhotep II in the west of Deir El-Bahari. Straightforward rockfall simulations for four orders of magnitude revealed runout trajectories and reach probabilities. At this point, these models present only a conservative first estimate but nonetheless prove their value in a comprehensive safeguarding strategy. Since our rockfall models do not account for fragmentation which is (i) evident for small magnitude rockfalls in the TLS data and (ii) most probable for larger failures, we
490 calibrated a granular flow simulation for two historic events at Deir El-Bahari. This calibration is based on rough volume estimations and fairly simple mechanics, however, (i) it provides easy-access validated friction parameters if needed for future event scenarios and (ii) at this point we do not have more reliable calibration information.

6.   Conclusion

The Temple of Hatshepsut, an engineering marvel from the fifteenth century BC and part of the UNESCO World Heritage
495 Site of Ancient Thebes, exhibits a unique architectural integration with Gebel Gurnah's rock mass, featuring ca. 100 m high, vertical cliffs with prominent rock tower structures. Due to its geomorphological setting, the temple complex and its visitors are exposed to potential gravitational mass movements. Therefore, a comprehensive and reliable natural hazard safeguarding strategy is required. For the first time, we successfully applied and combined three non-destructive measuring methods (TLS, InSAR, ambient vibrations) at an Egyptian World Heritage site to provide a proof of concept of an integrated methodological
500 approach and its capabilities towards a hazard anticipation and mitigation strategy. We show that

- The combination of TLS and InSAR at heritage sites in desert environments provides topographic change analysis with good spatial resolution and very high accuracy – higher than anticipated.
- Three local zones of significant deformation / surface change could be derived from the remote sensing data.
- Ambient vibration measurements have great potential at the site to close the time gap between the initiation of
505   potentially preparing rock wall instability and active process monitoring.
- Non-destructive and non-invasive methods are very capable and the right way to go at sensitive and prestigious cultural heritage sites.
- Straightforward rockfall and granular flow runout simulations provide valuable insights towards gravitational mass movement hazard assessment.
510 In summary, this study shows the remarkable potential of transferring established methods from mountainous regions to cultural heritage sites. We presented an integrated approach in a challenging climatic, geomorphological and archaeologically

sensitive environment, and produced the first event and impact analysis of gravitational mass movements at the Temple of Hatshepsut, providing vital data towards future risk assessment.

7. Data availability

515 The data is available upon reasonable request and authorization of the Egyptian Ministry of Antiquities.

8. Author contribution

HH and CG initiated the study and collaboration. BJ, MKe, MKr and MI designed the outline of the study in close cooperation with HH and CG. BJ, MI, ME, MKe, MKr, CG and HH conducted the field work in a joint effort. BJ analysed the TLS data, simulated runouts, and prepared and compiled the manuscript & figures with contributions from MI, ME and HH (Geological

520 Engineering and Rock mechanics), MKe (InSAR), AM (ambient vibration), JK (granular flow modelling) and revision and final approval from all authors.

9. Competing interests

One author is a member of the editorial board of the Copernicus journal *Earth Surface Dynamics*.

10. Acknowledgements

525 We thank the Supreme Council of Antiquities in general and the Antiquities Area 465 manager and employes at El-Deir El-Bahari region for their local support. We are very grateful for support from Dr. Alexander Schütze (LMU Institute for Egyptology and Coptology) providing access to literature and photographs. We thank Dr. Christian Haberland (GFZ Potsdam) for providing instruments for ambient vibration measurements. The team is grateful to the ScanPyramids mission for their consistent support.

11. Financial support

530

The study was funded by the TUM Global Incentive Fund 2022: HERITAGE - High-energy rockfall impact anticipation in a German-Egypt cooperation.

12. References

Abdallah, T. and Helal, H.: Risk evaluation of rock mass sliding in El-Deir El-Bahary valley, Luxor, Egypt, Bulletin of the
535   International Association of Engineering Geology-Bulletin de l'Association Internationale de Géologie de l'Ingénieur,
42, 3–9, https://doi.org/10.1007/BF02592614, 1990.

Abellán, A., Vilaplana, J. M., Calvet, J., García-Sellés, D., and Asensio, E.: Rockfall monitoring by Terrestrial Laser
Scanning – case study of the basaltic rock face at Castellfollit de la Roca (Catalonia, Spain), Nat. Hazards Earth Syst.
Sci., 11, 829–841, https://doi.org/10.5194/nhess-11-829-2011, 2011.

540   Abellán, A., Oppikofer, T., Jaboyedoff, M., Rosser, N. J., Lim, M., and Lato, M. J.: Terrestrial laser scanning of rock slope
instabilities, Earth surface processes and landforms, 39, 80–97, https://doi.org/10.1002/esp.3493, 2014.

Abellán, A., Calvet, J., Vilaplana, J. M., and Blanchard, J.: Detection and spatial prediction of rockfalls by means of
terrestrial laser scanner monitoring, Geomorphology, 119, 162–171, https://doi.org/10.1016/j.geomorph.2010.03.016,
2010.

545   Alcaíno-Olivares, R., Perras, M. A., Ziegler, M., and Maissen, J.: Cliff Stability at Tomb KV42 in the Valley of the Kings,
Egypt: A First Approach to Numerical Modelling and Site Investigation, 53rd U.S. Rock Mechanics/Geomechanics
Symposium, 2019.

Arnold, D.: Die Tempel Ägyptens: Götterwohnungen, Baudenkmäler, Kultstätten, Bechtermünz, Augsburg, 1996.

Aubry, M.-P., Dupuis, C., Berggren, W. A., Ghaly, H., Ward, D., King, C., Knox, R. W. O., Ouda, K., and Youssef, M.: The
550   role of geoarchaeology in the preservation and management of the Theban Necropolis, West Bank, Egypt, Proceedings of
the Yorkshire Geological Society, 61, 134–147, https://doi.org/10.1144/pygs2016-366, 2016.

Aubry, M.-P., Berggren, W. A., Dupuis, C., Ghaly, H., Ward, D., King, C., Knox, R. W. O., Ouda, K., Youssef, M., and
Galal, W. F.: Pharaonic necrostratigraphy: a review of geological and archaeological studies in the Theban Necropolis,
Luxor, West Bank, Egypt, Terra Nova, 21, 237–256, https://doi.org/10.1111/j.1365-3121.2009.00872.x, 2009.

555   Badawy, A., Abdel-Monem, S. M., Sakr, K., and Ali, S.: Seismicity and kinematic evolution of middle Egypt, Journal of
Geodynamics, 42, 28–37, https://doi.org/10.1016/j.jog.2006.04.003, 2006.

Beshr, A. M., Kamel Mohamed, A., ElGalladi, A., Gaber, A., and El-Baz, F.: Structural characteristics of the Qena Bend of
the Egyptian Nile River, using remote-sensing and geophysics, The Egyptian Journal of Remote Sensing and Space
Science, 24, 999–1011, https://doi.org/10.1016/j.ejrs.2021.11.005, 2021.

560   Carlà, T., Intrieri, E., Raspini, F., Bardi, F., Farina, P., Ferretti, A., Colombo, D., Novali, F., and Casagli, N.: Perspectives on
the prediction of catastrophic slope failures from satellite InSAR, Scientific reports, 9, 14137,
https://doi.org/10.1038/s41598-019-50792-y, 2019.

Caviezel, A., Lu, G., Demmel, S. E., Ringenbach, A., Bühler, Y., Christen, M., and Bartelt, P.: RAMMS:ROCKFALL - A
Modern 3-Dimensional Simulation Tool Calibrated on Real World Data, 53rd U.S. Rock Mechanics/Geomechanics
565   Symposium, 2019.

Caviezel, A., Ringenbach, A., Demmel, S. E., Dinneen, C. E., Krebs, N., Bühler, Y., Christen, M., Meyrat, G., Stoffel, A., Hafner, E., Eberhard, L. A., Rickenbach, D. von, Simmler, K., Mayer, P., Niklaus, P. S., Birchler, T., Aebi, T., Cavigelli, L., Schaffner, M., Rickli, S., Schnetzler, C., Magno, M., Benini, L., and Bartelt, P.: The relevance of rock shape over mass-implications for rockfall hazard assessments, Nature communications, 12, 5546, https://doi.org/10.1038/s41467-
570 021-25794-y, 2021.

Cesaro, G., Delmonaco, G., Khrisat, B., and Salis, S.: Geological Conservation Through Risk Mitigation and Public Awareness at the Siq of Petra, Jordan, in: Advancing Culture of Living with Landslides, edited by: Sassa, K., Mikoš, M., and Yin, Y., Springer International Publishing, Cham, 511–517, https://doi.org/10.1007/978-3-319-59469-9_45, 2017.

Chudzik, P., El Younsy, A.-R. M., Galal, W. F., and Salman, A. M.: Geological appraisal of the Theban cliff overhanging
575 the Hatshepsut temple at Deir el-Bahari, Polish Archaeology in the Mediterranean, 30, 275–295, 2022.

Collins, B. D. and Stock, G. M.: Rockfall triggering by cyclic thermal stressing of exfoliation fractures, Nature Geosci, 9, 395–400, https://doi.org/10.1038/ngeo2686, 2016.

Ćwiek, A.: Old and Middle Kingdom tradition in the Temple of Hatshepsut at Deir el-Bahari, Études et Travaux (Institut des Cultures Méditerranéennes et Orientales de l'Académie Polonaise des Sciences), 61–93, 2014.

580 Draebing, D., Mayer, T., McColl, S., Schlecker, M., and Jacobs, B.: Relief and elevation set limits on mountain size, https://doi.org/10.21203/rs.3.rs-5156557/v1, available at: https://www.researchsquare.com/article/rs-5156557/v1, 2024.

Draebing, D., Mayer, T., Jacobs, B., and McColl, S. T.: Alpine rockwall erosion patterns follow elevation-dependent climate trajectories, Commun Earth Environ, 3, 1–12, https://doi.org/10.1038/s43247-022-00348-2, available at: https://www.nature.com/articles/s43247-022-00348-2, 2022.

585 Dupuis, C., Aubry, M.-P., King, C., Knox, R. W., Berggren, W. A., Youssef, M., Galal, W. F., and Roche, M.: Genesis and geometry of tilted blocks in the Theban Hills, near Luxor (Upper Egypt), Journal of African Earth Sciences, 61, 245–267, https://doi.org/10.1016/j.jafrearsci.2011.06.001, 2011.

Erismann, T. H. and Abele, G.: Dynamics of rockslides and rockfalls: With 10 tables, Springer, Berlin, Heidelberg, 316 pp., 2001.

590 Falco, A. de, Resta, C., and Squeglia, N.: Satellite and on-site monitoring of subsidence for heritage preservation: A critical comparison from Piazza del Duomo in Pisa, Italy, in: Geotechnical Engineering for the Preservation of Monuments and Historic Sites III, edited by: Lancellotta, R., Viggiani, C., Flora, A., Silva, F. de, and Mele, L., CRC Press, London, 548–559, https://doi.org/10.1201/9781003308867-39, 2022.

Gado, T. A., El-Hagrsy, R. M., and Rashwan, I. M. H.: Projection of rainfall variability in Egypt by regional climate model
595 simulations, Journal of Water and Climate Change, 13, 2872–2894, https://doi.org/10.2166/wcc.2022.003, 2022.

Gaisecker, T. and Czerwonka-Schröder, D.: RIEGL V-Line Scanners for Permanent Monitoring Applications and integration capabilities into customers risk management, [White Paper], 2023.

Graber, A. and Santi, P.: Power law models for rockfall frequency-magnitude distributions: review and identification of
   factors that influence the scaling exponent, Geomorphology, 418, 108463,
600   https://doi.org/10.1016/j.geomorph.2022.108463, 2022.

Hartmeyer, I., Keuschnig, M., Delleske, R., Krautblatter, M., Lang, A., Schrott, L., Prasicek, G., and Otto, J.-C.: A 6-year
   lidar survey reveals enhanced rockwall retreat and modified rockfall magnitudes/frequencies in deglaciating cirques,
   Earth Surf. Dynam., 8, 753–768, https://doi.org/10.5194/esurf-8-753-2020, available at:
   https://esurf.copernicus.org/articles/8/753/2020/esurf-8-753-2020.html, 2020.

605   Hesthammer, J. and Fossen, H.: Evolution and geometries of gravitational collapse structures with examples from the
   Statfjord Field, northern North Sea, Marine and Petroleum Geology, 16, 259–281, 1999.

Hungr, O., Leroueil, S., and Picarelli, L.: The Varnes classification of landslide types, an update, Landslides, 11, 167–194,
   https://doi.org/10.1007/s10346-013-0436-y, available at: https://link.springer.com/article/10.1007/s10346-013-0436-y,
   2014.

610   Intrieri, E., Raspini, F., Fumagalli, A., Lu, P., Del Conte, S., Farina, P., Allievi, J., Ferretti, A., and Casagli, N.: The Maoxian
   landslide as seen from space: detecting precursors of failure with Sentinel-1 data, Landslides, 15, 123–133,
   https://doi.org/10.1007/s10346-017-0915-7, 2018.

Jackson, R. L., Green, I., and Marghitu, D. B.: Predicting the coefficient of restitution of impacting elastic-perfectly plastic
   spheres, Nonlinear Dyn, 60, 217–229, https://doi.org/10.1007/s11071-009-9591-z, 2010.

615   Jacobs, B. and Krautblatter, M.: LiDAR-basierte Quantifizierung von strukturellen Einflüssen auf Steinschlagaktivität in
   alpinen Kalksteinwänden., in: Fachsektionstage Geotechnik - Interdisziplinäres Forum: 6.-8. September 2017, Congress
   Centrum Würzburg Tagungsband, 2017.

Jacobs, B., Stammberger, V., and Krautblatter, M.: Geomorphic Hazard Mitigation in touristically developed Alpine Gorges:
   a Benchmark Study in the Höllental Gorge, Bavaria., in: INTERPRAEVENT 2024 Conference Proceedings, 2024.

620   Karakhanyan, A., Avagyan, A., and Sourouzian, H.: Archaeoseismological studies at the temple of Amenhotep III, Luxor,
   Egypt, Ancient Earthquakes, 471, 199, 2010.

Kenner, R., Gischig, V., Gojcic, Z., Quéau, Y., Kienholz, C., Figi, D., Thöny, R., and Bonanomi, Y.: The potential of point
   clouds for the analysis of rock kinematics in large slope instabilities: examples from the Swiss Alps: Brinzauls, Pizzo
   Cengalo and Spitze Stei, Landslides, 19, 1357–1377, https://doi.org/10.1007/s10346-022-01852-4, 2022.

625   King, C., Dupuis, C., Aubry, M.-P., Berggren, W. A., Knox, R. O., Galal, W. F., and Baele, J.-M.: Anatomy of a mountain:
   The Thebes Limestone Formation (Lower Eocene) at Gebel Gurnah, Luxor, Nile Valley, Upper Egypt, Journal of African
   Earth Sciences, 136, 61–108, https://doi.org/10.1016/j.jafrearsci.2017.05.008, 2017.

Klemm, R. and Klemm, D. D.: Steine und Steinbrüche im Alten Ägypten, Springer Berlin Heidelberg, Berlin, Heidelberg,
   1993.

630   Krautblatter, M. and Moser, M.: A nonlinear model coupling rockfall and rainfall intensity based on a four year
        measurement in a high Alpine rock wall (Reintal, German Alps), Nat. Hazards Earth Syst. Sci., 9, 1425–1432,
        https://doi.org/10.5194/nhess-9-1425-2009, available at: https://nhess.copernicus.org/articles/9/1425/2009/, 2009.

        Lague, D., Brodu, N., and Leroux, J.: Accurate 3D comparison of complex topography with terrestrial laser scanner:
        Application to the Rangitikei canyon (N-Z), ISPRS Journal of Photogrammetry and Remote Sensing, 82, 10–26,

635   https://doi.org/10.1016/j.isprsjprs.2013.04.009, 2013.

        Leinauer, J., Dietze, M., Knapp, S., Scandroglio, R., Jokel, M., and Krautblatter, M.: How water, temperature, and seismicity
        control the preconditioning of massive rock slope failure (Hochvogel), Earth Surf. Dynam., 12, 1027–1048,
        https://doi.org/10.5194/esurf-12-1027-2024, 2024.

        Lipinska, J.: Deir El-Bahari II: The Temple of Thuthmosis III: the Architecture, 1977.

640   Lipińska, J.: 'Deir el-Bahari-Temple of Thutmosis III', Seventy Years of Polish Archaeology in Egypt, 105–114, 2007.

        Margottini, C., Bobrowsky, P., Gigli, G., Ruther, H., Spizzichino, D., and Vlcko, J.: Rupestrian World Heritage Sites:
        Instability Investigation and Sustainable Mitigation, in: Advancing Culture of Living with Landslides, edited by: Sassa,
        K., Mikoš, M., and Yin, Y., Springer International Publishing, Cham, 23–50, https://doi.org/10.1007/978-3-319-59469-
        9_2, 2017.

645   Marija, L., Martin, Z., Jordan, A., and Matthew, P.: Rockfall susceptibility and runout in the Valley of the Kings, Natural
        Hazards, 110, 451–485, https://doi.org/10.1007/s11069-021-04954-9, 2022.

        Massaro, L., Forte, G., Falco, M. de, Rauseo, F., and Santo, A.: Rockfall source identification and trajectory analysis from
        UAV-based data in volcano-tectonic areas: a case study from Ischia Island, Southern Italy, Bulletin of the International
        Association of Engineering Geology-Bulletin de l'Association Internationale de Géologie de l'Ingénieur, 83,

650   https://doi.org/10.1007/s10064-024-03569-1, 2024.

        Matasci, B., Stock, G. M., Jaboyedoff, M., Carrea, D., Collins, B. D., Guérin, A., Matasci, G., and Ravanel, L.: Assessing
        rockfall susceptibility in steep and overhanging slopes using three-dimensional analysis of failure mechanisms,
        Landslides, 15, 859–878, https://doi.org/10.1007/s10346-017-0911-y, available at:
        https://link.springer.com/article/10.1007/s10346-017-0911-y, 2018.

655   Mendler, A., Rada Erazo, J. D., Ismael, M., Ezzy, M., Jacobs, B., Haberland, C., Krautblatter, M., Helal, H., and Grosse, C.
        U.: Vibration Monitoring of the Rock Formation Above the Hatshepsut Temple, eJNDT, 29,
        https://doi.org/10.58286/29649, 2024.

        Mohadjer, S., Ehlers, T. A., Nettesheim, M., Ott, M. B., Glotzbach, C., and Drews, R.: Temporal variations in rockfall and
        rock-wall retreat rates in a deglaciated valley over the past 11 k.y, Geology, 48, 594–598,

660   https://doi.org/10.1130/G47092.1, 2020.

        Nakamura, Y.: A method for dynamic characteristics estimation of subsurface using microtremor on the ground surface, OR
        or RTR1, 30, 1989.

        Naville, E.: The Temple of Deir El Bahari: Part III, Offices of the Egypt exploration fund, 1913.

Naville, E.: The Temple of Deir El Bahari: Part I, Offices of the Egypt exploration fund, 1907.

665   Naville, E.: The Temple of Deir El Bahari: Its Plan, its Founders, and its first Explorers, Offices of the Egypt exploration fund, 1894.

Noël, F., Nordang, S. F., Jaboyedoff, M., Digout, M., Guerin, A., Locat, J., and Matasci, B.: Comparing Flow-R, Rockyfor3D and RAMMS to Rockfalls from the Mel de la Niva Mountain: A Benchmarking Exercise, Geosciences, 13, 200, https://doi.org/10.3390/geosciences13070200, 2023.

670   Pawlikowski, M. and Wasilewski, M.: Some remarks on jointing in the Theban limestones in the region of Deir el-Bahari, Egypt, Geologia/Akademia Górniczo-Hutnicza im. Stanisława Staszica w Krakowie, 30, 47–56, 2004.

Pechnikov, A.: PyGMTSAR (Python InSAR), https://doi.org/10.5281/zenodo.7725131, available at: https://insar.dev, 2024.

RAMMS AG: RAMMS:DEBRISFLOW User Manual: User Manual v1.8 Debrisflow, https://ramms.ch/wp-content/uploads/RAMMS_DBF_Manual.pdf, last access: 28 March 2025, 2024a.

675   RAMMS AG: RAMMS:ROCKFALL User Manual: User Manual v1.8 Rockfall, https://ramms.ch/wp-content/uploads/RAMMS_ROCK2_Manual.pdf, last access: 28 March 2025, 2024b.

Rosser, N. J., Brain, M. J., Petley, D. N., Lim, M., and Norman, E. C.: Coastline retreat via progressive failure of rocky coastal cliffs, Geology, 41, 939–942, https://doi.org/10.1130/G34371.1, 2013.

Said, R.: The Geology of Egypt, Routledge, 2017.

680   Santos Delgado, G., J. Martínez Rubio, Serafín Monterrubio Pérez, and María del Carmen Yenes Varela: Control de Movimientos con Técnica de Láser Escáner 3D en Laderas Inestables de laCuenca del Duero. El Caso de Aguilarejos (Valladolid), VII Simposio Nacional sobre Taludes y Laderas Inestables: Barcelona, 27-30 de octubre de 2009, 243–255, available at: https://dialnet.unirioja.es/servlet/articulo?codigo=8801358, 2009.

Solari, L., Ciampalini, A., Raspini, F., Bianchini, S., and Moretti, S.: PSInSAR Analysis in the Pisa Urban Area (Italy): A

685   Case Study of Subsidence Related to Stratigraphical Factors and Urbanization, Remote Sensing, 8, 120, https://doi.org/10.3390/rs8020120, 2016.

Strunden, J., Ehlers, T. A., Brehm, D., and Nettesheim, M.: Spatial and temporal variations in rockfall determined from TLS measurements in a deglaciated valley, Switzerland, JGR Earth Surface, 120, 1251–1273, https://doi.org/10.1002/2014JF003274, 2015.

690   UNESCO World Heritage: Ancient Thebes with its Necropolis, https://whc.unesco.org/en/list/87/, last access: 28 March 2025, 2025.

van Overschee, P. and Moor, B. de: A unifying theorem for three subspace system identification algorithms, Automatica, 31, 1853–1864, https://doi.org/10.1016/0005-1098(95)00072-0, available at: https://www.sciencedirect.com/science/article/pii/0005109895000720, 1995.

695   Weber, S., Fäh, D., Beutel, J., Faillettaz, J., Gruber, S., and Vieli, A.: Ambient seismic vibrations in steep bedrock permafrost used to infer variations of ice-fill in fractures, Earth and Planetary Science Letters, 501, 119–127, https://doi.org/10.1016/j.epsl.2018.08.042, 2018.

Williams, J. G., Rosser, N. J., Hardy, R. J., Brain, M. J., and Afana, A. A.: Optimising 4-D surface change detection: an approach for capturing rockfall magnitude–frequency, Earth Surf. Dynam., 6, 101–119, https://doi.org/10.5194/esurf-6-101-2018, available at: https://esurf.copernicus.org/articles/6/101/2018/, 2018.

700

Winiwarter, L., Anders, K., Czerwonka-Schröder, D., and Höfle, B.: Full four-dimensional change analysis of topographic point cloud time series using Kalman filtering, Earth Surf. Dynam., 11, 593–613, https://doi.org/10.5194/esurf-11-593-2023, 2023.

Winlock, H. E.: Excavations At Deir El Bahari): 1911-1931, The MacMillan Company, New York, 1942.

705 Witte, B. and Schmidt, H.: Vermessungskunde und Grundlagen der Statistik für das Bauwesen, 6., überarb. Aufl., Wichmann, Heidelberg, 678 pp., 2006.

Zachert, K.: Preliminary report on the activities of the Polish Cliff Mission working at Deir El-Bahari between 28th January and 12th March 2014, available at: https://www.academia.edu/8581023/Preliminary_report_on_the_activities_of_the_Polish_Cliff_Mission_working_at_De

710 ir_El_Bahari_between_28th_January_and_12th_March_2014, 2014a.

Zachert, K.: Preliminary report on the results of the works done by the Polish Cliff Mission at Deir el-Bahari in the season: October–December 2014, available at: https://www.academia.edu/12746709/Preliminary_report_on_the_results_of_the_works_done_by_the_Polish_Cliff_Miss ion_at_Deir_el_Bahari_in_the_season_October_December_2014, 2014b.

715 Zachert, K.: Preliminary report on the works of the Polish Cliff Mission at Deir el-Bahari in the season: 22 September – 10 December 2015, available at: https://www.academia.edu/20032515/Preliminary_report_on_the_works_of_the_Polish_Cliff_Mission_at_Deir_el_Baha ri_in_the_season_22_September_10_December_2015, 2014c.